JOURNAL OF MAGNETIC RESONANCE **125,** 153–158 (1997)
ARTICLE NO. MN961074

PGSE NMR Measurements of Convection in a Capillary

B. MANZ, J. D. SEYMOUR, AND P. T. CALLAGHAN

Department of Physics, Massey University, Palmerston North, New Zealand

Received November 8, 1996

Since the first experiments performed by Stejskal and Tanner (*1*), the pulsed-gradient spin-echo (PGSE) method has been employed to measure correlated and uncorrelated motion in a number of systems. For a spin ensemble undergoing random Brownian motion, the Stejskal–Tanner plot of the spin-echo attenuation function provides the self-diffusion coefficient of the sample. If the molecular motion is restricted, for example, due to confinement of the molecules within pores, diffraction-like coherence effects can be observed in the spin-echo decay. Recently, the existence of PGSE NMR diffraction effects has been demonstrated in porous-media flow (*2*). In that case, the coherence effects arose because of the spatial correlation of the pores. A different type of interference experiment associated with flow is one where a sample contains spins whose host molecules travel with differing velocities. The resulting PGSE NMR signal thus results from a superposition of signals with differing phase shifts. Because of the simple Fourier relationship which lies at the heart of the method, this signal may be directly related to the velocity distribution by Fourier inversion (*3*).

Here we describe such an interference experiment, in this case due to the velocity distribution associated with stationary convection arising from a vertical temperature gradient. The earliest systematic experiments on convectional flow are those of Bénard (*4, 5*). He showed that there exists a critical temperature gradient beyond which convectional instability is established, and that the resulting motions have a stationary cellular character. The conditions may be characterized by the so-called Rayleigh number (*6*) R_a given by

$$R_a = \frac{g\alpha\Delta T}{\kappa\nu}\, d^3, \qquad [1]$$

where g is the acceleration due to gravity, α, ν, and κ are the coefficient of thermal expansion, kinematic viscosity, and thermal diffusivity of the fluid, respectively, ΔT is the vertical temperature difference across the sample, and d is the thickness of the fluid layer. Convection results if R_a exceeds a critical value R_c, approximately 1700 for a cell with infinite horizontal dimensions (*7*). In practice, the critical Rayleigh number depends on the geometry of the container holding the sample liquid and the boundary conditions. Charlson and Sani (*8, 9*) analyzed the situation for convection in cylindrical containers, with both conducting and insulating walls, at different aspect ratios Γ, the ratio of the sample radius to its height. In the case of interest here, Γ has a value of 0.06, and R_c is on the order of 10^7 (*9*).

In previous studies, the velocity distributions in convection cells were measured by visually recording the motion of suspended particles or by magnetic resonance imaging (*10, 11*). This study shows that the PGSE experiment provides an alternative method for the investigation of convection driven flows. Our work is relevant to the results of Goux *et al.* (*12*) whose PGSE experiments exhibited an increase in the apparent self-diffusion coefficient with the onset of convection.

Unlike imaging experiments, the PGSE NMR method for examining velocity distributions employs a single gradient only. Another variant of the method is the two-dimensional velocity-exchange experiment (VEXSY) (*13*). There, the displacements Z_1 and Z_2 are made over two well-defined time intervals, which are themselves separated by a mixing time, τ_m. Z_1 and Z_2 correspond to the classical spectral domains f_1 and f_2, and a subset of molecules traveling at a constant velocity has identical displacements, thus contributing to points on the diagonal of the two-dimensional spectrum in (Z_1, Z_2) space. A migration of spins from one region in the displacement spectrum to another over the mixing time leads to cross peaks. By varying the mixing time, the molecular velocities can be correlated. We shall demonstrate that the VEXSY experiment is well suited to the demonstration of stationarity in convective flow.

The basic two-pulse PGSE pulse sequence is shown in Fig. 1a. If $\bar{P}_s(\mathbf{R},\Delta)$ is the average probability for a spin to have a dynamic displacement $\mathbf{R}$ over the time Δ, the echo attenuation function $E(\mathbf{q})$ can be written as (*14*)

$$E(\mathbf{q}) = \int \bar{P}_s(\mathbf{R},\Delta)\exp(i2\pi\mathbf{q}\cdot\mathbf{R})\, d\mathbf{R}, \qquad [2]$$

where $\mathbf{q} = (2\pi)^{-1}\,\gamma\delta g$.

$\bar{P}_s(\mathbf{R},\Delta)$ can be obtained from the velocity distribution, for example by using the dynamic spin-echo experiment shown in Fig. 1b. The echo signal $S(\mathbf{k}, \mathbf{q})$ is then given by

1090-7807/97 $25.00

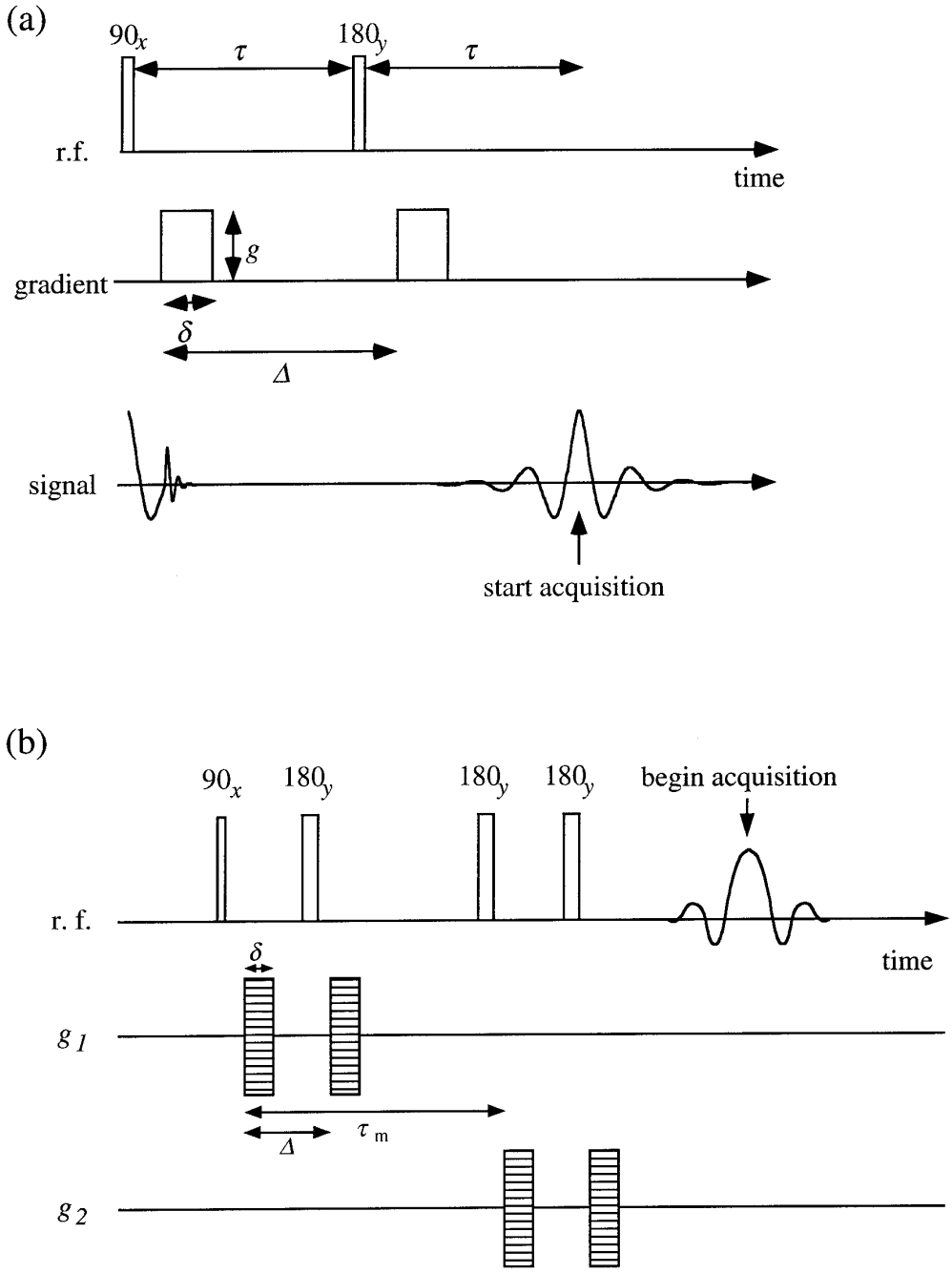

FIG. 1. (a) The PGSE pulse sequence. (b) The VEXSY pulse sequence. (c) The dynamic spin-echo pulse sequence.

$$S(\mathbf{k}, \mathbf{q}) = \rho(\mathbf{r})\exp(i2\pi\mathbf{k}\cdot\mathbf{r}) \times \int P_s(\mathbf{R}, \Delta)\exp(i2\pi\mathbf{q}\cdot\mathbf{R})d\mathbf{R}d\mathbf{r}, \quad [3]$$

$$\bar{P}_s(\mathbf{R}, \Delta) = \iint S(\mathbf{k}, \mathbf{q})\exp(-i\pi\mathbf{k}\cdot\mathbf{r}) \times \exp(-i2\pi\mathbf{q}\cdot\mathbf{R})d\mathbf{k}d\mathbf{q}. \quad [4]$$

where $\mathbf{k} = (2\pi)^{-1}\gamma\mathbf{G}t$, and $\rho(\mathbf{r})$ is the proton density distribution in the sample. Allowing $\rho(\mathbf{r})$ to be uniform across the sample the velocity propagator in each pixel $\bar{P}_s(\mathbf{R}, \Delta)$ can be obtained by inverse Fourier transformation of Eq. [3]:

The experiments described here utilized a 5% w/w polystyrene/cyclohexane solution (M_w = 127,000 g mol^{-1}) inside a standard 4 mm o.d. NMR tube. They formed part of a larger study on polystyrene diffusion in which convection effects led to severe perturbations. These effects were subse-

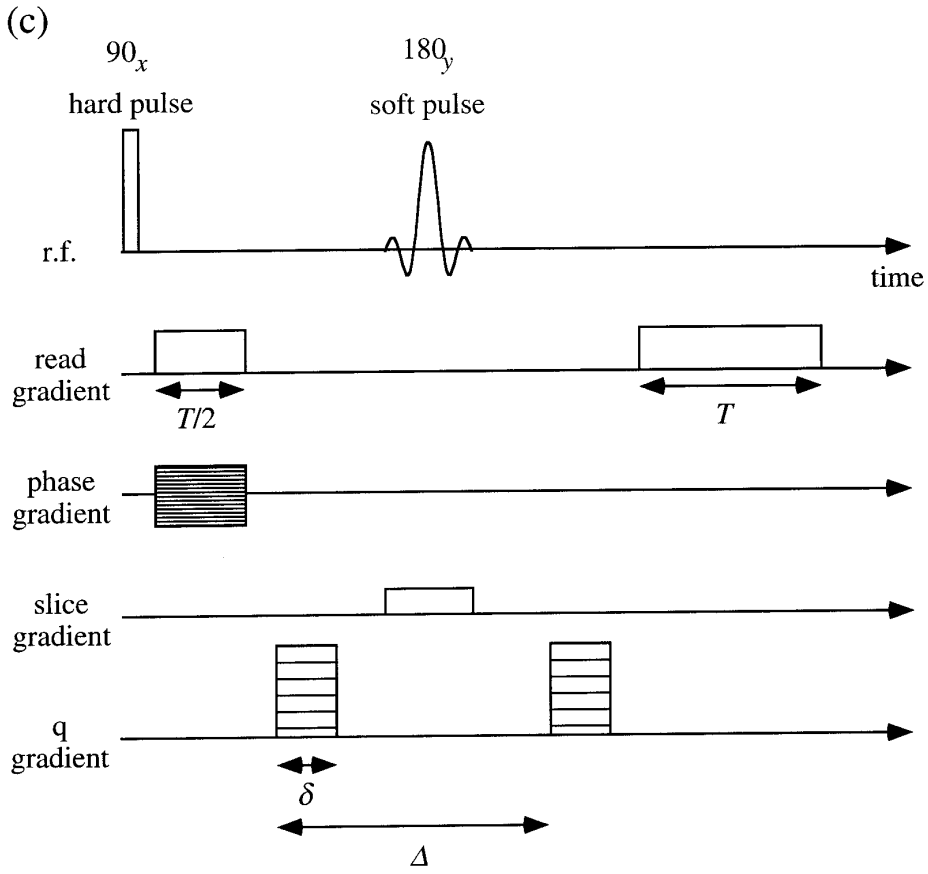

FIG. 1—*Continued*

quently suppressed by surrounding the polymer sample with a jacket of low-viscosity fluid. However, the unsuppressed convection is of intrinsic interest, partly for its own sake and partly because of the need to recognize the signature for such disturbances when carrying out PGSE diffusion studies at elevated temperatures.

The sample height was 25 mm, giving an aspect ratio of $\Gamma = 0.06$. PGSE NMR measurements were carried out using a Bruker AMX 300 spectrometer. Pulsed gradients were generated both with a microimaging probe and a home-built high-gradient probe developed for the measurement of self-diffusion of high-molar-mass polymer solutions. The maximum achievable gradient in this latter probe was 5 T m^{-1}. No slice selection was used. The sample was heated inside the RF coil from below by a stream of 50°C hot air, and the vertical temperature difference across the sample was measured to be 4 K. The viscosity of the polymer solution is $\eta = 1.43 \times 10^{-3}$ Pa s (*15*), and using the literature values of α and κ, for cyclohexane (*16*), the Rayleigh number is estimated to be $R_a \approx 10^7$, which is on the same order as R_c for the present aspect ratio.

The PGSE experiments were performed using the total signal arising from the rapidly diffusing solvent and slowly diffusing solute. The two-pulse PGSE experiment employs strong gradient pulses, and while the signal is dominated by the polymer protons, some contribution from the solvent exists at the lowest q values. However, this contribution has vanished at q values sufficient to observe coherence effects. The gradient pulse duration δ was increased in 16 q-encoding steps from 3 to 10.5 ms. The gradient amplitude was $g = 0.36$ T m^{-1}, while the delay Δ between the q-encoding gradient pulses was 40 ms. The data are displayed in Fig. 2, both as a Stejskal–Tanner plot and as a plot of $E(q)$ vs q. It is obvious that the data points exhibit pronounced minima and maxima akin to a diffraction pattern (*17*). The first interference minimum appears at a value of q which is the inverse of the maximum dynamic displacement of the molecules over the time Δ. We note that these interference effects arise from a different cause than the flow diffraction in porous media observed by Seymour and Callaghan (*2*) and are more akin to the non-Gaussian Stejskal–Tanner plots obtained by Hayward *et al.* (*3*) in their study of Poiseuille and plug flow in a pipe. In our case however, the diffraction patterns arise from a completely different flow profile.

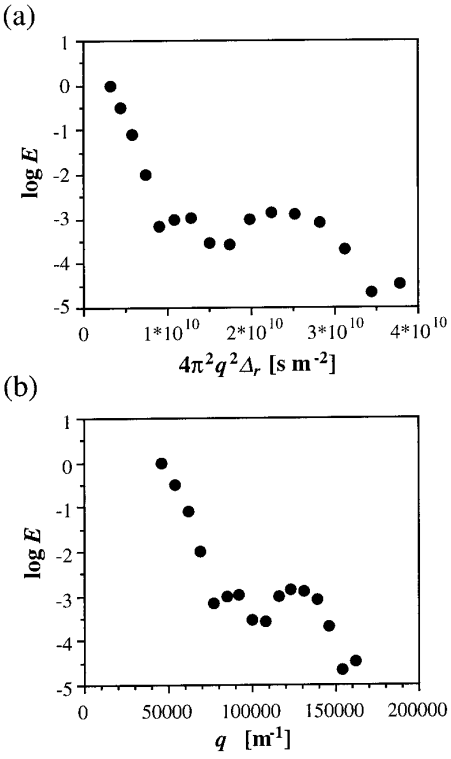

FIG. 2. (a) A Stejskal–Tanner plot of the echo attenuation from a PGSE experiment using a polymer solution undergoing convectional flow as a sample. Note the pronounced minima and maxima which have a close resemblance to a diffraction pattern. (b) The same data as in (a), but plotted vs q.

Furthermore, unlike the case of porous media flow, the instantaneous flow profile for convection can be directly measured by NMR imaging techniques.

Imaging experiments require a degree of stationarity in the flow structure in order that motion remain consistent over the time taken to spatially encode the data. In order to test the stationarity condition, we turn now to the VEXSY technique. The pulse sequence is shown in Fig. 1b. The VEXSY spectra were recorded using 64^2 phase encoding steps with a gradient pulse duration of $\delta = 2.5$ ms, gradient pulse amplitude of 2.25 T m^{-1}, and pulse separation $\Delta =$ 15 ms. The mixing times were $\tau_m = 25$ and 125 ms, respectively. Because there is no read gradient applied, the method is chemical-shift sensitive. Figures 3a and 3b show the VEXSY spectra of the solvent for the two different mixing times. Both spectra are essentially identical, both are diagonal indicating no velocity exchange over the mixing time, and both exhibit broadening due to Brownian motion. This origin of the broadening becomes evident when comparing the VEXSY spectrum of the polymer shown in Fig. 3c with the VEXSY spectrum for the solvent. The polymer distribution is much narrower due to the smaller self-diffusion coefficient.

Given the stationary nature of the velocity distribution, the imaging of velocity becomes straightforward. We have used the dynamic spin-echo pulse sequence shown in Fig. 1c. In order to directly compare the results from the velocity image with those obtained using the PGSE method, no slice selection was used. The duration of the q-encoding gradient pulses was 2 ms, the amplitude was incremented in 16 steps from 0 to 0.72 T m^{-1}, and the separation between the q pulses was 40 ms. The velocity image is shown in Fig. 4a. From this, the average displacement propagator $\bar{P}_s(\mathbf{R}, \Delta)$ can be obtained by calculating a histogram of displacement values. This is shown in Fig. 4b. With Eq. [2], the function $E(q)$ can be calculated using a numerical FT of the data points shown in Fig. 4b. This function $E(q)$ is shown in Fig. 5, both as a Stejskal–Tanner plot and as the diffraction

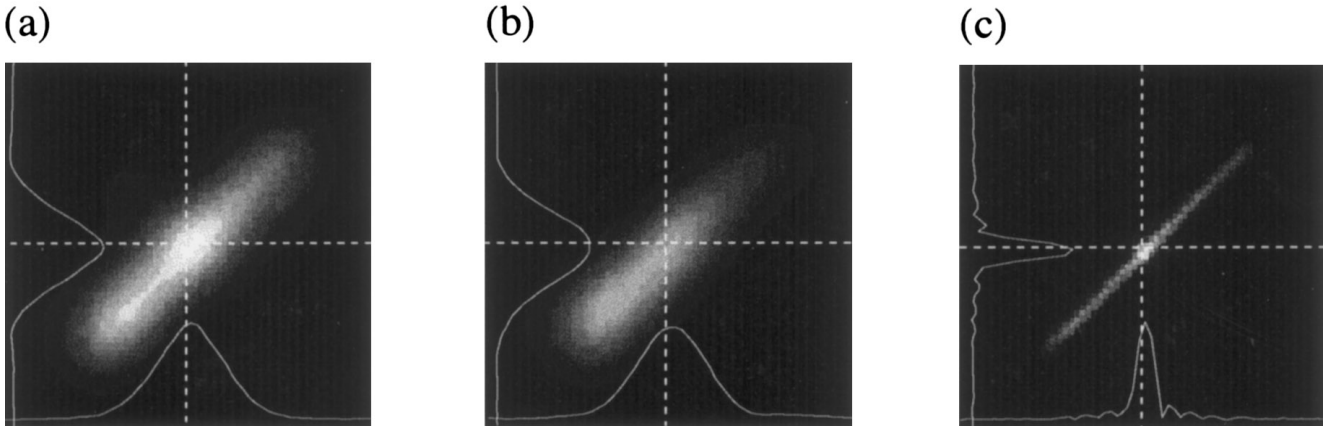

FIG. 3. The two-dimensional VEXSY spectra of a polymer solution undergoing convectional flow. The displacement field of view is 133 μm. The VEXSY spectra of the solvent for mixing times of 25 and 125 ms are shown in (a) and (b), respectively. The VEXSY spectrum for the polymer is shown in (c) for a mixing time of 25 ms.

plot $E(q)$ vs q. The key features of the diffraction plot correspond nicely with the PGSE data shown in Fig. 2.

It is clear that coherence effects in simple PGSE experiments can be used to extract information about the flow profiles. But in order to interpret the echo attenuation plot in terms of a simple model for the velocity distribution, the VEXSY test of stationarity is crucial. A major advantage of both methods is that only one gradient direction is required. We stress here the difference between interference effects caused by phase coherences in stationary flow from diffraction effects arising from spatial correlations in porous media, for example, those observed in diffusive- and flow-diffraction experiments. These latter experiments exhibit randomized VEXSY spectra with strongly off-diagonal character.

In the present instance, we have been able to demonstrate the application of both methods to the study of convective flow, providing independent evidence for the convection cell by means of NMR imaging. The signature for convection which we have demonstrated in the PGSE NMR experiment should prove useful in the identification of artifacts in future diffusion studies under conditions of elevated temperature.

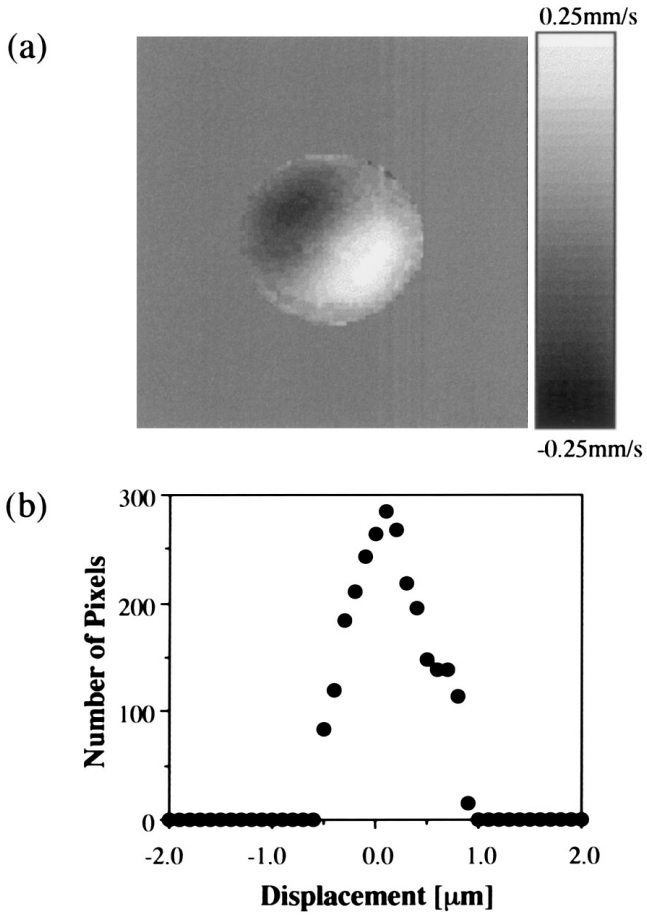

FIG. 4. (a) A velocity image of a polymer solution in a 4 mm o.d. NMR tube which is heated from below. (b) The displacement propagator extracted from the velocity image in (a).

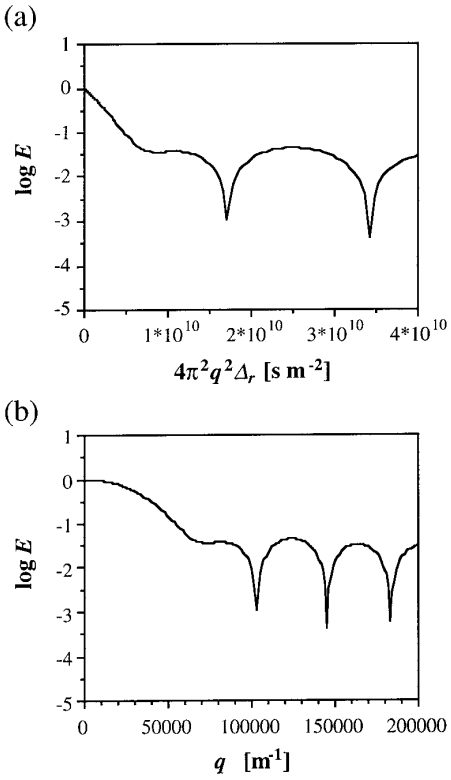

FIG. 5. The Fourier transform of the velocity propagator displayed in Fig. 4b plotted as a Stejskal–Tanner plot (a) and vs q (b).

ACKNOWLEDGMENTS

B.M. acknowledges financial support under the ''DAAD-Doktorandenstipendien aus Mitteln des zweiten Hochschulsonderprogramms'' from the German Academic Exchange Service while J.D.S. acknowledges support from an NSF International Program Postdoctoral Fellowship, Grant INT-9500445. The authors are grateful to the New Zealand Foundation for Research, Science and Technology for major funding.

REFERENCES

1. E. O. Stejskal, *J. Chem. Phys.* **43,** 3597–3603 (1965).
2. J. D. Seymour, and P. T. Callaghan, *J. Magn. Reson. A* **122,** 90–93 (1996).
3. R. J. Hayward, K. J. Packer, and D. J. Tomlinson, *Mol. Phys.* **23,** 1083–1102 (1972).
4. H. Bénard, *Rev. Sci. Pures Appl.* **11,** 1261–1271 and 1309–1328 (1900).
5. H. Bénard, *Ann. Chim. Phys.* **23,** 62–144 (1901).
6. Lord Rayleigh. *Philos. Mag.* **32,** 529–546 (1916).
7. S. Chandrasekhar, ''Hydrodynamic and Hydromagnetic Stability,'' Clarendon Press, Oxford, 1961.

8. G. S. Charlson, and R. L. Sani, *Int. J. Heat Mass Transfer* **13,** 1479–1496 (1970).
9. G. S. Charlson, and R. L. Sani, *Int. J. Heat Mass Transfer* **14,** 2157–2160 (1971).
10. S. J. Gibbs, T. A. Carpenter, and L. D. Hall, *J. Magn. Reson. A* **105,** 209–214 (1993).
11. J. Weis, R. Kimmich, and H.-P. Müller, *Magn. Reson. Imaging* **14,** 319–327 (1996).
12. W. J. Goux, L. A. Verkruyse, and S. J. Salter, *J. Magn. Reson.* **88,** 609–614 (1990).
13. P. T. Callaghan, and B. Manz, *J. Magn. Reson. A* **106,** 260–265 (1994).
14. P. T. Callaghan, ''Principles of Nuclear Magnetic Resonance Microscopy,'' Clarendon Press, Oxford, 1991.
15. L. A. Papazian, *Polymer* **10,** 399–420 (1969).
16. D. R. Lide, ''Handbook of Chemistry and Physics,'' CRC Press, New York, 1995.
17. P. T. Callaghan, A. Coy, D. MacGowan, K. J. Packer, and F. O. Zelaya, *Nature* **351,** 467–469 (1991).